DASA-11.026

R 377

Technical Report

AN ABSOLUTE MEASUREMENT OF THERMAL NEUTRON ALBEDO FOR SEVERAL MATERIALS

May 1965

U. S. NAVAL CIVIL ENGINEERING LABORATORY

Port Hueneme, California

AN ABSOLUTE MEASUREMENT OF THERMAL NEUTRON ALBEDO FOR SEVERAL MATERIALS

Y-F008-08-05-201, DASA-11.026

Type C

by

Duane Robert Doty

ABSTRACT

Albedo is a concept which has proved useful in the calculation of the penetration of nuclear weapons radiation through a shelter entranceway. The application of the albedo approach to describe the behavior of neutrons impinging upon various materials is the subject of this report.

Values of thermal neutron albedo for lead, iron, paraffin, aluminum, carbon, and high-density concrete were measured, using the nuclear reactor of the University of California at Los Angeles. The results are in reasonable agreement with theoretical calculations. Verification of the angular dependence of neutron scattering was attempted, but with only partial success.

Albedo as a function of thickness of the scattering material was measured for paraffin, carbon, and aluminum. The results essentially conform with theory.

The possibility of using a simple empirical formula for albedo calculations of thermal-neutron streaming through shelter ducts is apparent.

This work sponsored by the Defense Atomic Support Agency.

OBJECTIVE

The work reported herein was performed in connection with Task Y-F008-08-05-201, Fundamental Studies of Gamma and Neutron Shielding Properties of Shelters. The objective of this task is to improve existing knowledge on gamma and neutron shielding properties of shelters and to verify experimentally, where necessary, theoretical information developed in the field, in order to fill in gaps in nuclear shielding knowledge.

As a part of this task, the present work was undertaken to determine thermal neutron albedo values for several materials because of the importance of albedo in calculations of neutron streaming through ducted entranceways.

APPROACH

Because of its lack of charge, the interactions of a neutron with matter can be quite complex, since these reactions occur on a nuclear scale. What happens when a plane wave of neutrons encounters some object may accordingly be difficult to describe. Approximations can be made on the basis of complex models, such as those used in transport theory and diffusion theory, but these techniques are often extremely cumbersome to apply. Thus, a simple model is desired to indicate how neutrons are reflected from materials and how neutrons stream in complicated geometries.

One fruitful approach is the albedo concept.[1,2,3,4,5] The following pages indicate the usefulness of albedo when considering a beam of neutrons reflected by a plane scattering surface. The validity of this approach is discussed, and values of albedo as a function of angle are given for lead, heavy concrete, and iron. Values of albedo for a given angle and several thicknesses are given for carbon, paraffin, and aluminum.

THEORY

Albedo

When a neutron impinges upon a surface of material, it may be scattered, be absorbed, or pass through. Which reaction dominates is a complicated function of the material and the neutron energy, involving an energy-dependent cross section for scattering and absorption, and the density of the scattering material. For a large number of common construction materials, a reasonable number of neutrons are back-scattered, or re-emitted. If this re-emission were known, one could easily calculate, for example, the number of neutrons that could survive a bend in a duct. Knowledge thus gained would have immediate use in shelter entranceway and reactor shielding design.

Scattering Geometry

Consider a plane element of scattering material of area A exposed to some incident flux N_o (neutrons/cm^2-sec) incident at a polar angle θ_o, as shown in Figure 1. A perfectly reflecting material which scatters isotropically would distribute the incident flux uniformly over a solid angle of 2π, and thus the backscattered flux at distance R from the material would be

$$N = \frac{N_o \cos\theta_o A}{2\pi R^2} \tag{1}$$

The $\cos\theta_o$ term was inserted to account for the fact that the orientation of the elemental scattering area with respect to the source affects the flux incident upon its surface. No azimuthal dependence has been inserted since none would be expected for thermal energies. Other investigations have shown this to be the case.[5,6]

It is desired to know how N varies with θ_o and θ, the polar angles of incidence and reflection, respectively. The angular dependence can be described for comparison with experiment by insertion of an albedo factor in Equation 1. Thus,

$$N(\theta) = \frac{N_o \cos\theta_o A}{R^2} \alpha(\theta, \theta_o) \tag{2}$$

where α, the albedo, modifies the scattered distribution of neutrons. An important experimental consideration is that the detector must look at a small section of the scattering material in order to avoid edge effects.

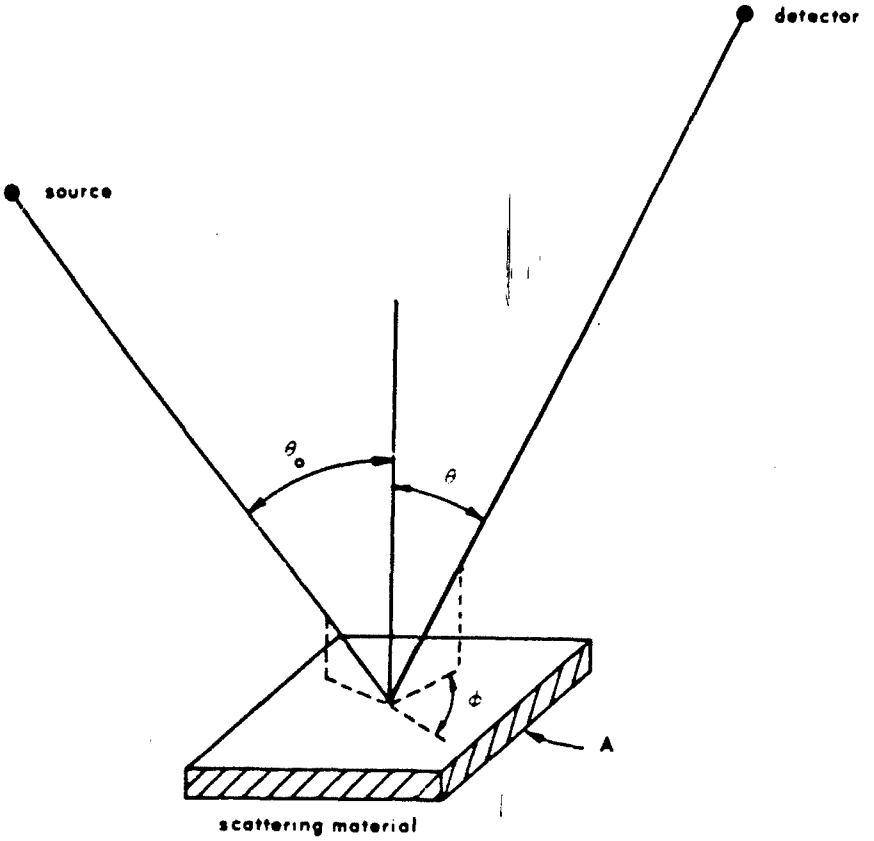

Figure 1. Scattering geometry.

The nomenclature for Equation 2 is unfortunate in that the 2π factor is generally absorbed into α. If this were not the case, then an albedo could be crudely related to a reflection coefficient; and when $\alpha = 1$, total reflection would occur, corresponding to a 2π source of secondary re-emitted neutrons. In our case this would be represented by $\alpha = 1/2\pi = 0.159$. It should also be noted that an $\alpha(\theta) > 0.159$ at some angle θ does not indicate more neutrons are emitted than absorbed but that the distribution is peaked, favoring emission in the direction θ. The only requirement for total reflection is that

$$\int_0^{2\pi} \int_0^1 \alpha(\theta)\, d\phi\, d(\cos\theta) = 1$$

Detector

The main requirement for an experimental measurement of angular neutron albedo is that neutrons be detected directionally. For these first measurements, thermal neutrons were chosen since they can easily be absorbed or collimated by cadmium. A boron trifioride (BF_3) counter was selected as a detector because of its sensitivity to neutrons and its ability to differentiate from other radiation.

Cadmium foil surrounded the detector and projected 10.75 inches forward so that only a small area of the scatterer was observed by the counter, as is shown in Figure 2. Each elemental area of the detector surface dS observes an area A' of the scattering surface area A. Thus $A' \approx \pi b^2 R^2/Z^2$ and is approximately independent of the position of dS on the detector's surface. The approximation becomes very close when $b^2 \ll Z^2$. In the present case, $b^2 = 0.25$ and $Z^2 = 116$.

To determine the effectiveness of the collimated detector in counting neutrons emitted from the plane surface, let us define

C = the number of neutrons through the front face of the detector per unit time

n = the number of neutrons emitted from the scattering surface area A per unit time

dC' = the number of neutrons through dS from dA'

dC = the number of neutrons through dS from A'

dA' = the differential area on the scattering surface seen by the detector surface

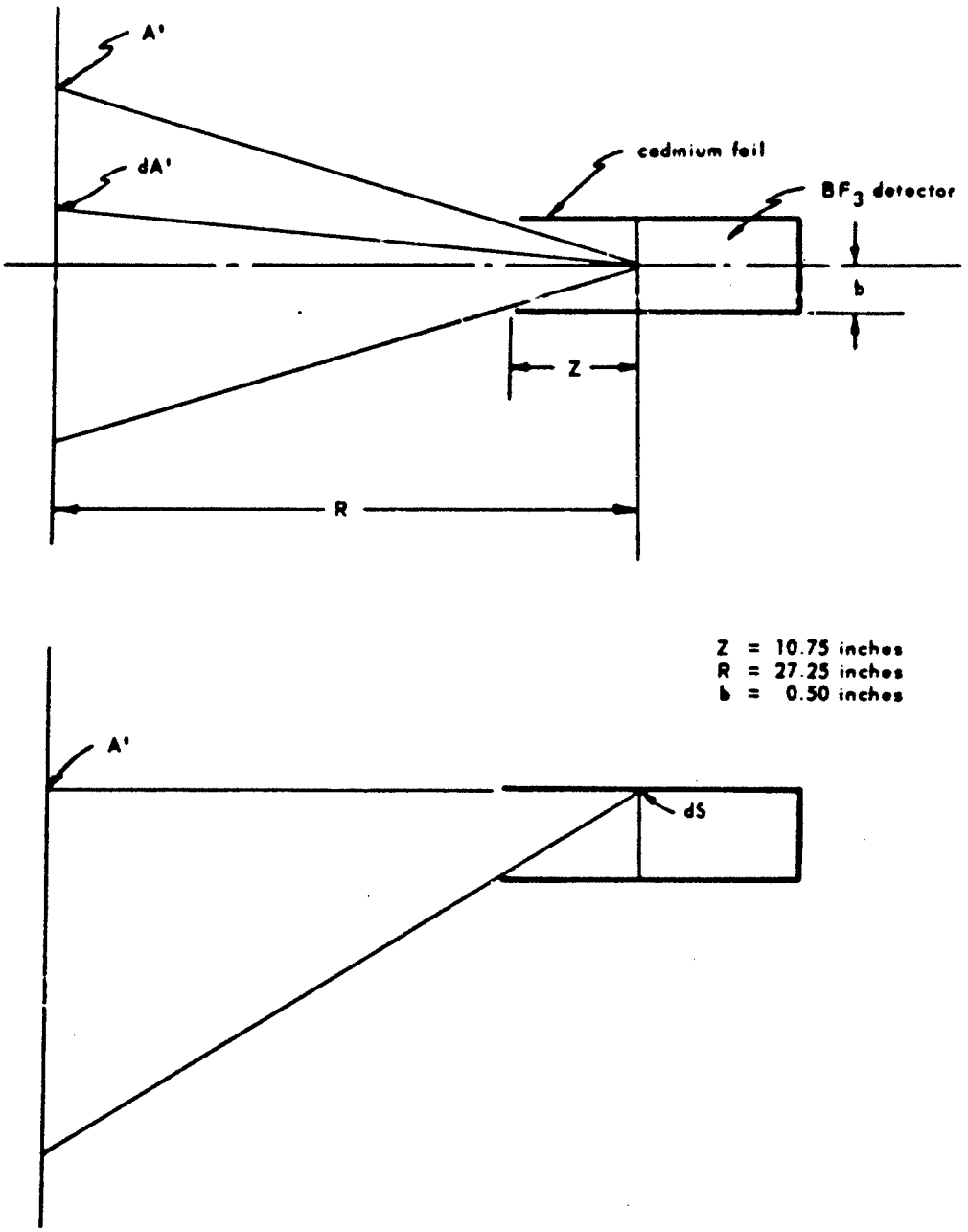

Figure 2. Areas A' of scattering surface seen from elements of detector surface dS at different positions on detector surface.

Thus we have

$$dC' = \frac{n\,dA'}{2\pi\rho^2}$$

for a 2π emitter of secondary neutrons. If $\rho^2 \approx R^2 >> b^2$, then

$$dC' = \frac{n\,dA'}{2\pi R^2}\,dS \qquad \text{and} \qquad dC = \frac{n\,A'}{2\pi R^2}\,dS$$

Since

$$A' = \frac{\pi b^2 R^2}{Z^2}$$

then

$$dC = \frac{n\left(\frac{\pi b^2}{Z^2}\,R^2\right)dS}{2\pi R^2} = \frac{n b^2}{2 Z^2}\,dS$$

Again dC is defined as the number of neutrons through dS from the area of the scatterer seen by dS per unit time interval. This is exactly true only when each dA' is at the same distance from dS.

The number of neutrons per unit detector area per unit time passing the surface is

$$\frac{dC}{dS} = \frac{n b^2}{2 Z^2}$$

thus, the <u>total</u> number of neutrons passing the detector surface is

$$C = \int \frac{dC}{dS}\,dS = \frac{dC}{dS}\,\pi b^2 = \frac{n\pi b^4}{2 Z^2} \qquad (3)$$

In order to evaluate albedo we must determine the effective area A_{eff} of the scatterer observed by the collimated detector. The number of neutrons per unit area per unit time at the detector is

$$N = \frac{n A_{eff}}{2\pi R^2}$$

But this is also equal to

$$\frac{C}{\pi b^2} = \frac{n A_{eff}}{2\pi R^2}$$

giving

$$A_{eff} = \frac{2R^2}{b^2} \frac{C}{n}$$

Remembering that $C/n = \pi b^4/2Z^2$, we have

$$A_{eff} = \frac{2R^2}{b^2} \frac{\pi b^4}{2Z^2} = \frac{\pi R^2 b^2}{Z^2} \tag{4}$$

For the general case the detector is not normal to the scattering plane and there is an angle θ between the collimator axis and the normal to the scattering surface, as in Figure 3. For this case the expression for the effective area is similar to the above, but modified by a $\cos\theta$ dependence in the denominator:

$$A_{eff} = \frac{\pi R^2 b^2}{Z^2 \cos\theta} \tag{5}$$

Flux Determination

It remains to evaluate N and N_o in Equation 2. This in itself is the problem of the experiment and is generally insolvable except for special cases. Problems of counter efficiency, energy change, and statistical fluctuations usually set a large error on the results.

In this experiment neutrons were thermalized before scattering so that no energy change would occur. Thus, energy-dependent effects on the BF_3 tube were avoided.

The incident flux N_o was found by placing the counter, with its cadmium shield pulled back 10.75 inches, parallel to and facing into the incoming beam at the position the scatterer would usually occupy, as is shown in Figure 4. The counting

rate C_o of the detector is proportional to the neutron flux N_o. Next, the collimator was moved forward 10.75 inches beyond the detector face, which was again pointed at the scattering position. Then the scatterer was inserted, angles were measured, and a count, $C(\theta)$, proportional to the flux $N(\theta)$ was obtained. The same proportional factor enters here as above, and since N/N_o occurs in the albedo equation, (2), these factors cancel. Thus,

$$\alpha(\theta, \theta_o) = \frac{N}{N_o} \frac{R^2}{\cos\theta_o A} = \frac{C}{C_o} \frac{R^2}{\cos\theta_o A_{eff}} = \frac{C}{C_o} \frac{\cos\theta}{\cos\theta_o} \frac{Z^2}{\pi b^2} \qquad (6)$$

This solution is possible since the divergences of the scattered and incident neutrons are the same within the accuracy of the experiment. If this were not the case, an uncalculable efficiency factor would enter into the result. N/N_o, representing the flux ratio, is now equal to C/C_o, the counts per unit time ratio, and α may be calculated knowing this ratio and the geometry.

DATA

Tables I, II, and III following the text display detector counting rates as a function of θ for several values of θ_o for lead, high-density concrete, and iron. Table IV displays counting rate versus thickness for paraffin, aluminum, and reactor-grade carbon (with less than 1/10 ppm of boron). Table V displays counting rates for 1-inch cubes of carbon, aluminum, paraffin, and lead. This data was corrected for extraneous radiation such as background gammas and fast neutrons by placing a cadmium shield over the collimator and counting in the various angular positions. At all times the back of the detector was shielded for no neutron entry. The scatterer was placed 54 inches from the thermal port of the reactor, and all scattering was coplanar.

It is of interest to note that for certain angles the counter was actually in the neutron beam and the flux read was lower due to the absorption of neutrons that contributed to N_o. See, for example, $\theta_o = 45^\circ$ and $\theta = -45^\circ$ in Table II.

COMPUTATIONS

Figures 5, 6, and 7 show $\alpha(\theta_o, \theta)$ for lead, concrete, and iron. The error bars shown represent standard deviations based on the square root of the counts. Table VI displays albedo values for paraffin, aluminum, and carbon. Table VII lists albedo values for 1-inch cubes of lead, aluminum, carbon, and paraffin. These latter values were computed employing the formula

$$N = \frac{N_o}{R^2} \alpha A$$

Here A is 1 square inch. The cadmium shield was no longer needed for collimation, but was retained to help reduce correction for extraneously scattered background neutrons. No angular measurements were made since for such a small scattering element (with dimensions on the order of or less than a scattering length), θ and θ_o have no real meaning since no surface is defined.

DISCUSSION OF RESULTS

If the reflection of thermal neutrons from a scattering area were completely isotropic, $\alpha(\theta, \theta_o)$ would show no variation with θ. In most cases the dependence on θ is more marked. This can be accounted for by assuming the finite scattering plane shows edge effects for large values of θ and θ_o. This problem cannot be resolved because as θ approaches 90^o an infinite amount of scatterer is observed. Thus, even at 60^o the edge effects of a finite scattering slab would cause α to drop. Another difficulty is to hold N_o constant over a large area. N_o versus lateral displacement for various distances from the reactor port is shown in Figure 8. Another problem arises when θ_o is varied. The flux falls off from the reactor core inversely as R^2 and is not constant over an appreciable extent of the scatterer unless the two are strictly perpendicular. This is shown in Figure 9. Note the flux buildup at the wall from the backscattered neutrons. If the experimental albedo values are accepted as true, they would indicate preferential backward scattering, since for paraffin and carbon the experimental albedo values are above the theoretical values.

The magnitudes of a measured albedo are a function of its thickness. The experimentally determined albedo value, α_{expt}, should approach the theoretical value, α_{theory}, when the scattering thickness is several scattering lengths ($1/\Sigma_s$), where Σ_s is the macroscopic scattering cross section. A feel for the size of α may be obtained by tabulating the absorption and scattering cross sections, as is done in Table VIII. When σ_s/σ_a is a large number ($>>1$), α should approach the limiting value of $\alpha_{max\ theory} = 0.159$. Theoretical values of α from Rafalski[7] for a semi-infinite slab wall of various ratios of σ_s/σ_a are included in Table VIII. These values were obtained by dividing Rafalski's values by 2π and assuming his albedo to be isotropic. If α_{expt} values are below these values, it is probably because the scattering slab is too thin. Scattering lengths are listed in Table VIII for the various materials used. The concrete values are from an Oak Ridge National Laboratory report[5] for portland concrete.

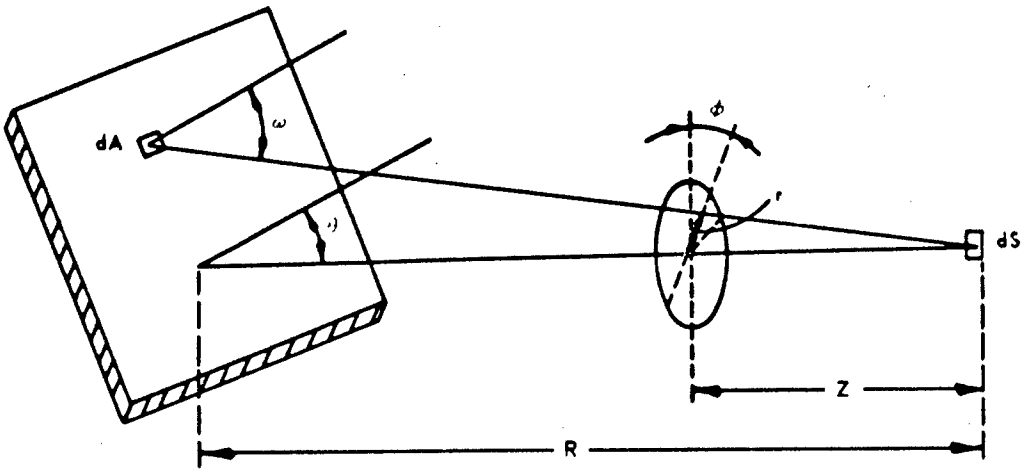

$$dA' = \frac{(r\,dr\,d\phi)\rho^2}{(r^2 + Z^2)\cos\omega}$$

$$\int dC'\,dS = \int \frac{n\,r\,dr\,d\phi\,\rho^2\,dS}{2\pi\rho^2(r^2 + Z^2)\cos\omega}$$

$$C = \frac{n\pi b^4}{2Z^2\cos\theta} \quad \text{for } r^2 \ll Z^2 \text{ and } \cos\omega \approx \cos\theta$$

$$\text{and } A_{eff} = \frac{\pi R^2 b^2}{Z^2\cos\theta}$$

Figure 3. Detector geometry for the general case.

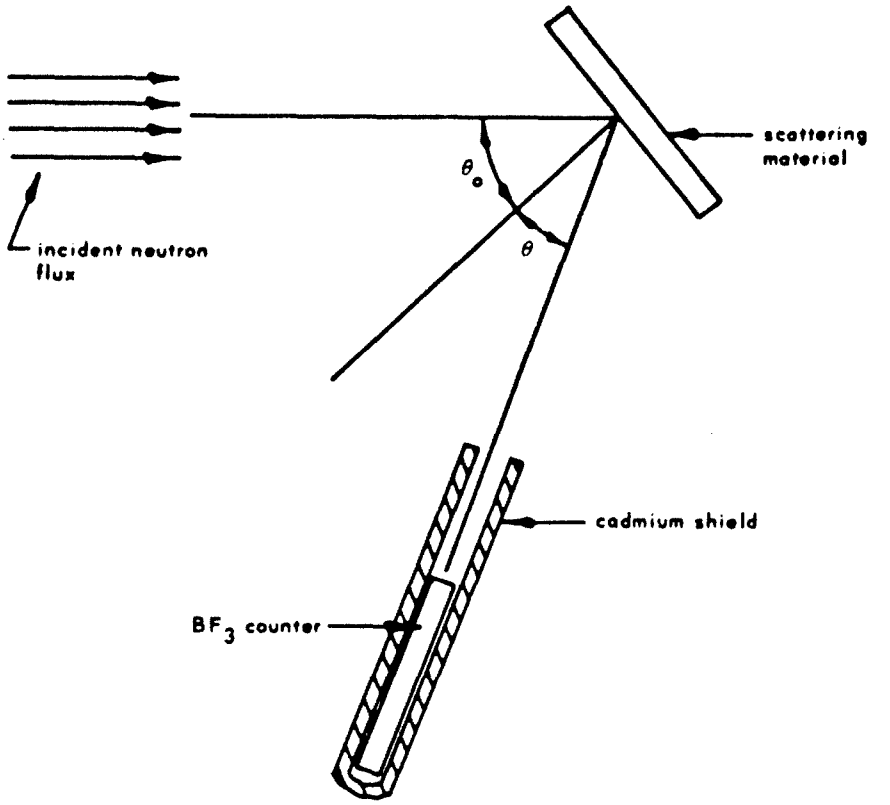

(a) Obtaining $C(\theta, \theta_o)$ for a given material and reactor power

(b) Obtaining C_o for a given reactor power

Figure 4. Geometry and collimator positions for obtaining C and C_o.

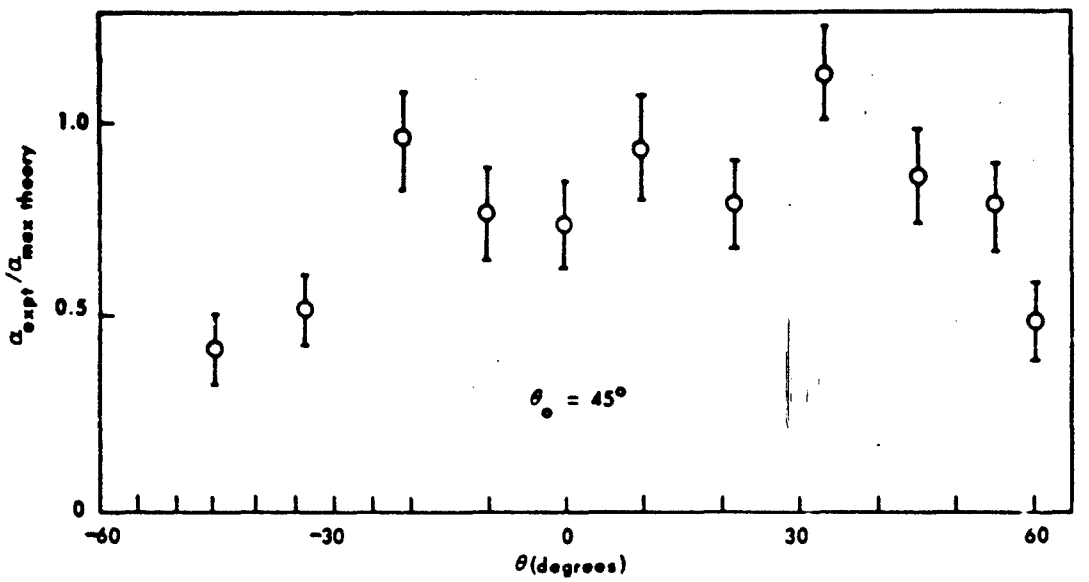

$\alpha_{max\ theory}$ = 0.159

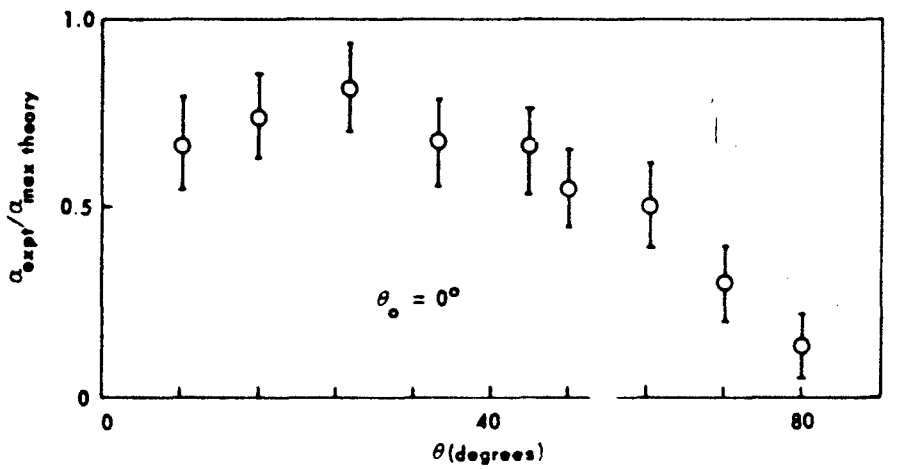

Figure 5. Albedo values for lead.

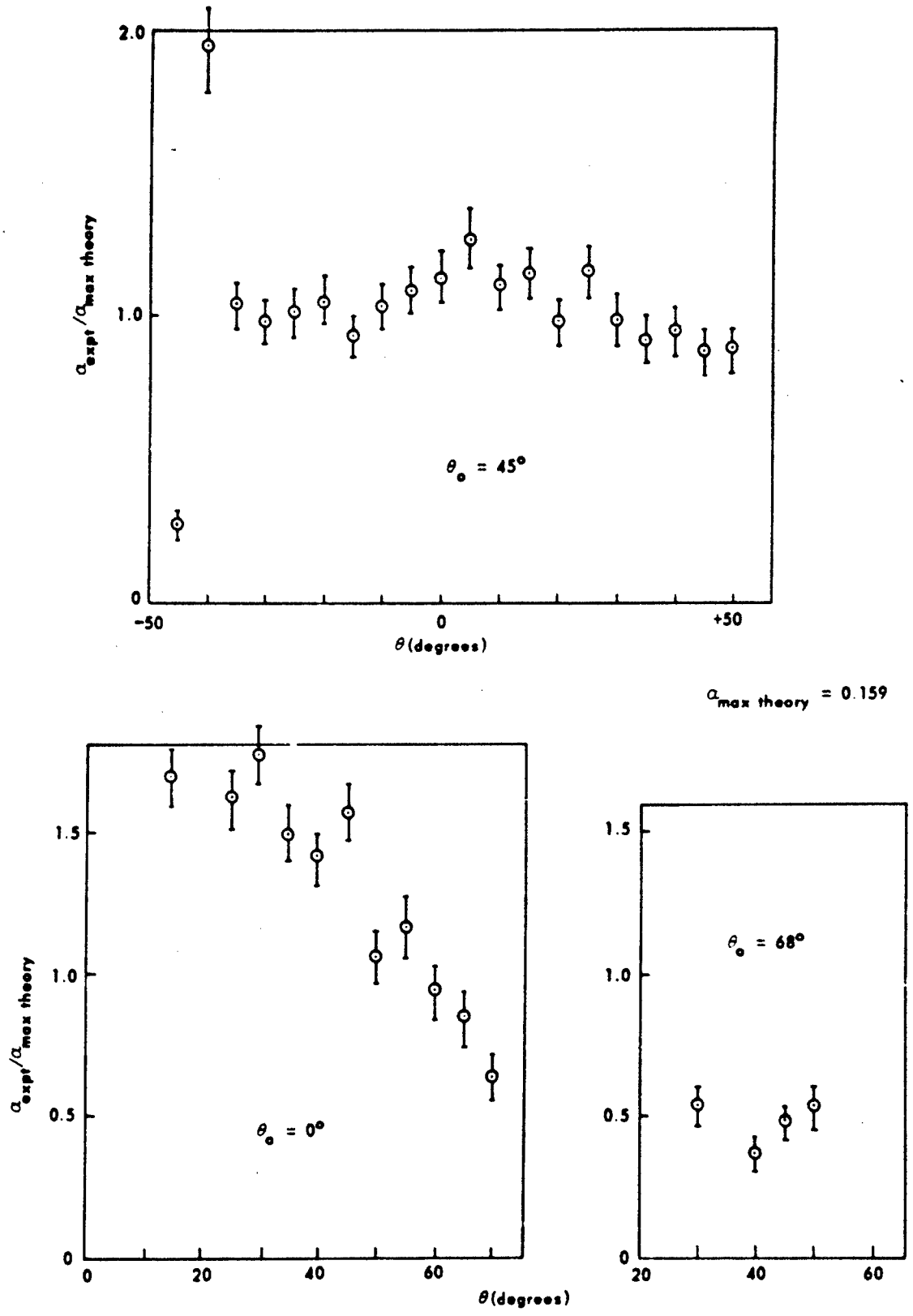

Figure 6. Albedo values for high-density concrete.

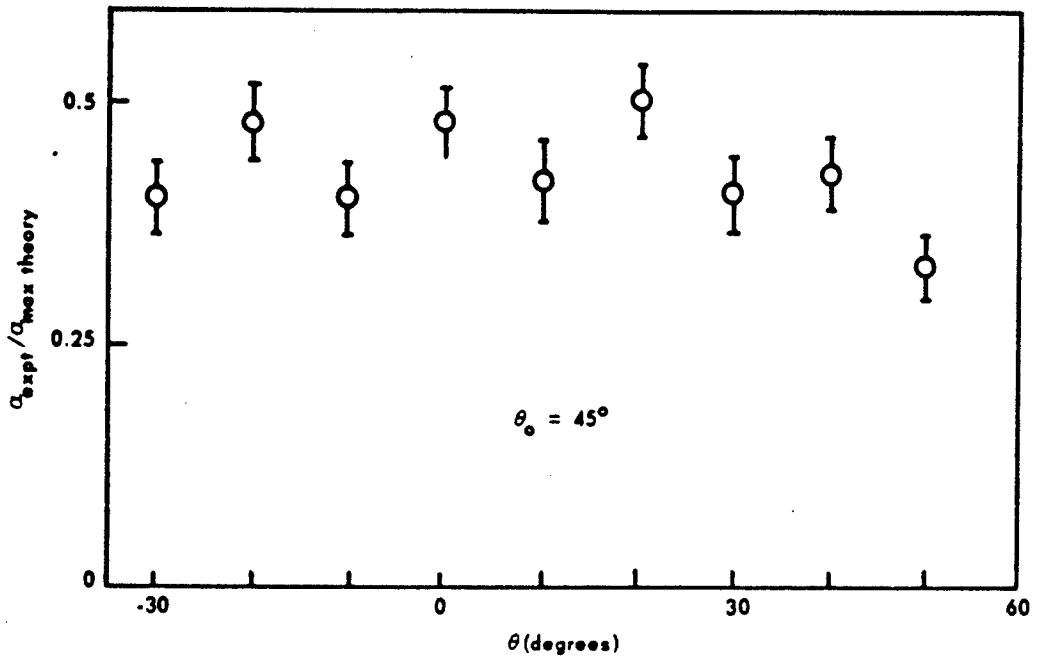

$\alpha_{max\ theory}$ = 0.159

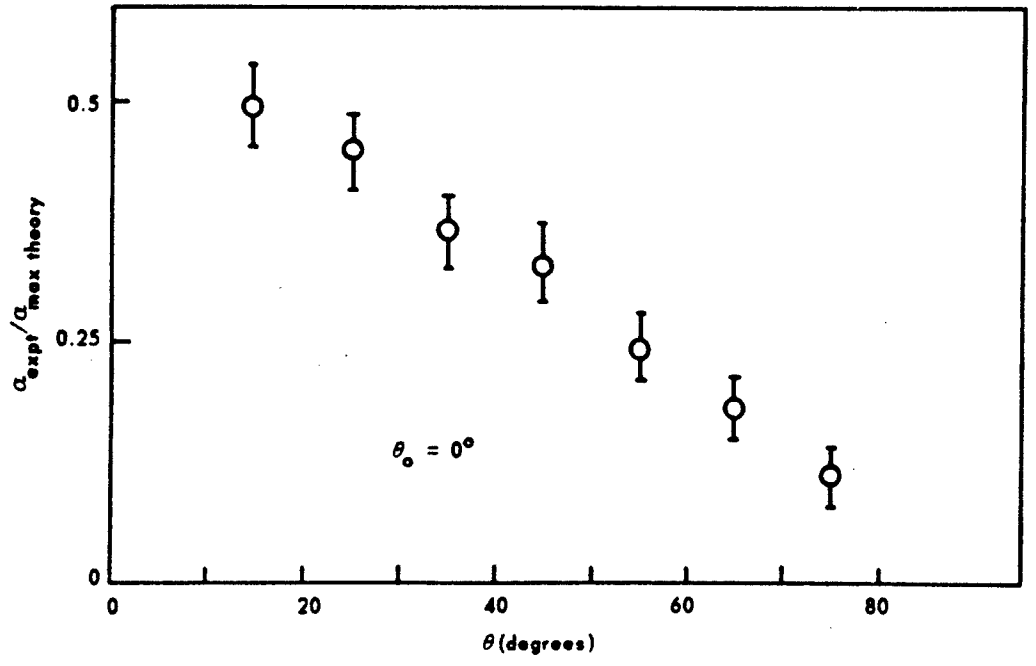

Figure 7. Albedo values for iron.

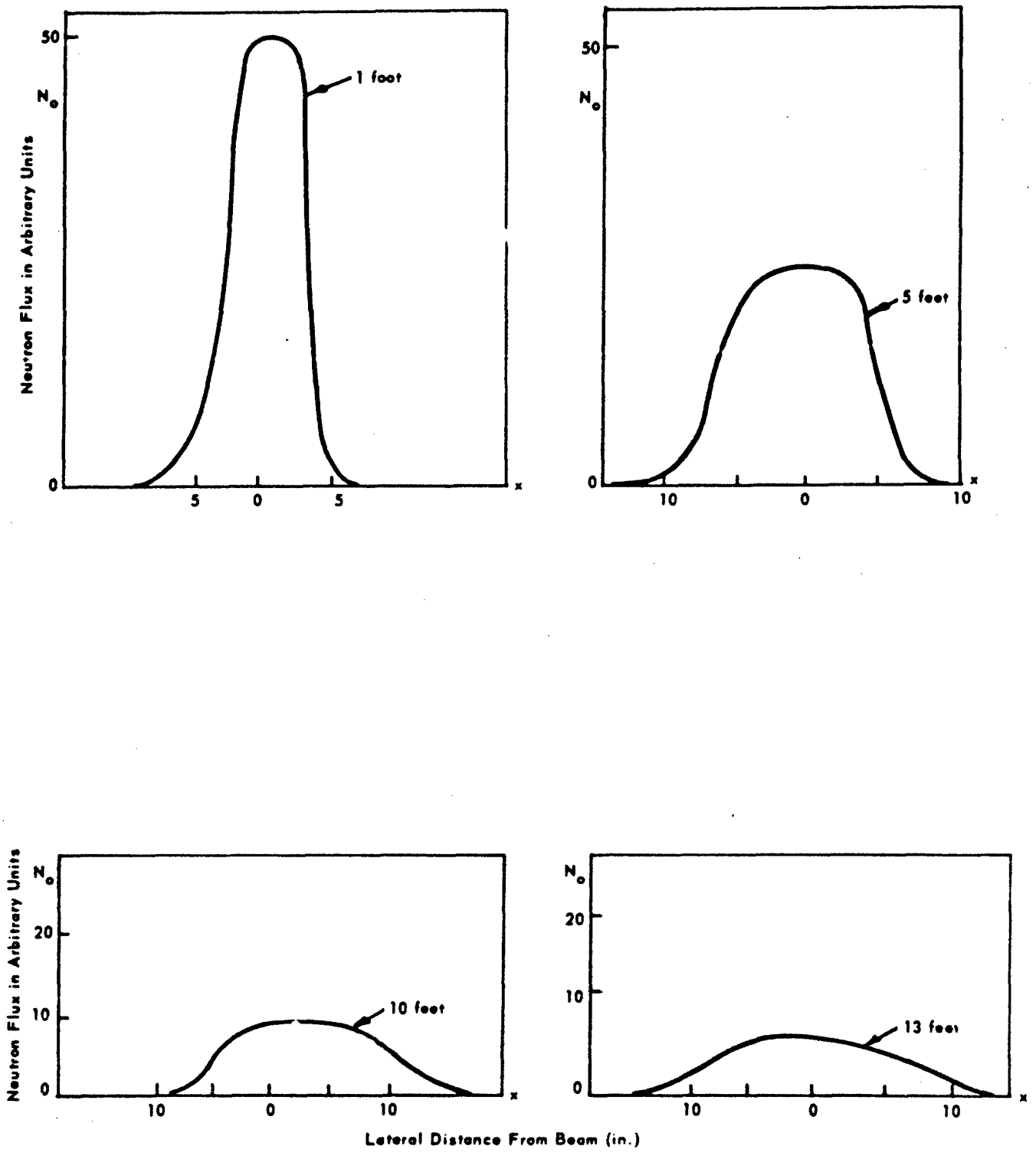

Figure 8. Beam expansion versus distance from reactor port.

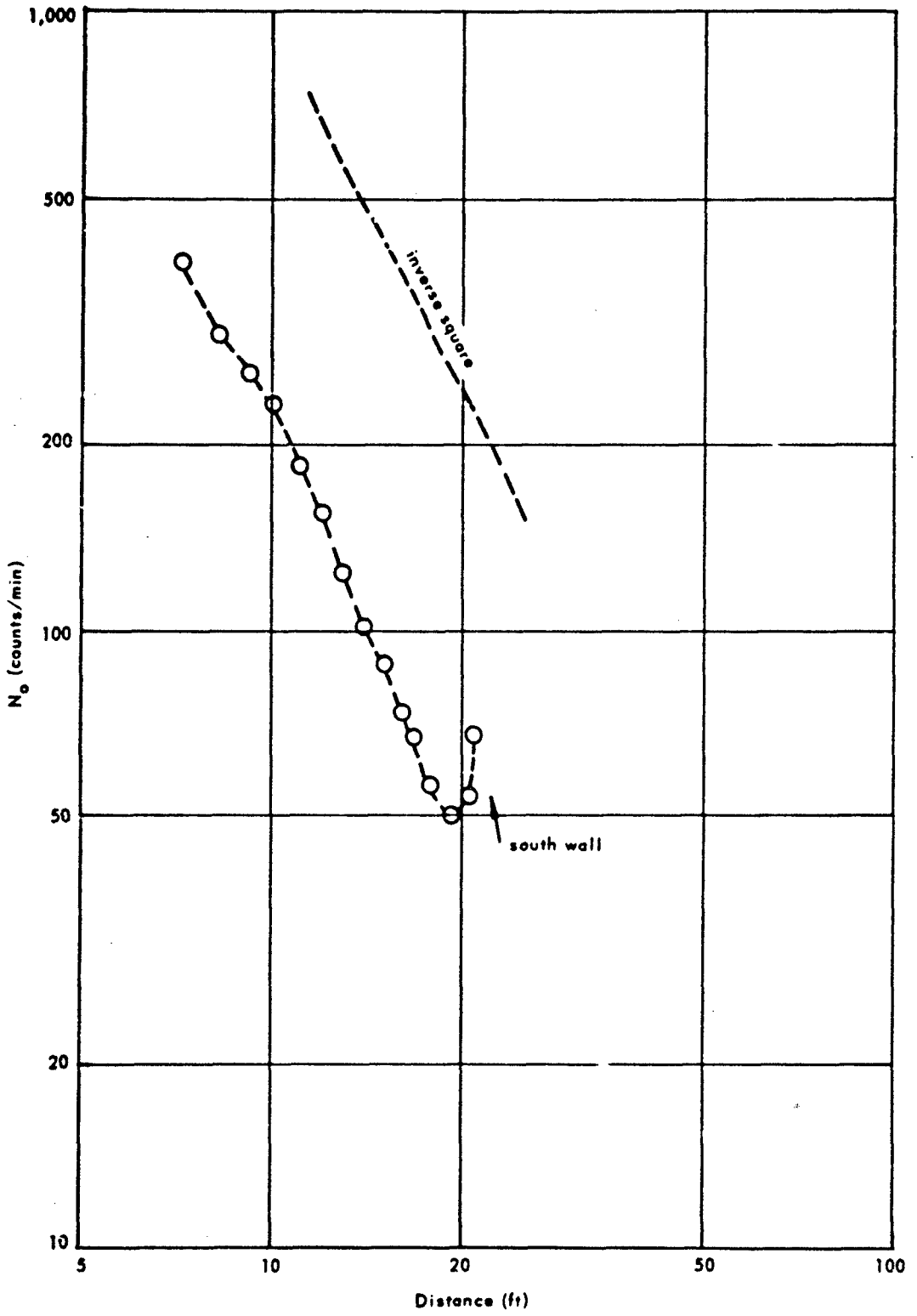

Figure 9. Variation of neutron flux with distance from reactor port.

Figure 10 shows α versus thickness of the scattering slab for paraffin, aluminum, and a theoretical case. For aluminum the scattering thickness is much less than a scattering length, and α is a linearly rising function of thickness. The paraffin is in the opposite case where the asymptotic limit has been reached and there is no variation of α with thickness other than statistical fluctuations. In both cases the albedo value for the 1-inch cube has been inserted, and it is rather surprising that for aluminum the albedo value fits in well with the other data. These results are more reasonable when the distance of one scattering length is considered — about 5 inches for aluminum and 1/10 inch for paraffin. The maximum thickness of the aluminum was less than one-half of a scattering length, and therefore there was no flux buildup in the scattering material. This means edge effects would not tend to lower the albedo value. On the other hand, the 1-inch paraffin cube was almost ten scattering lengths in size, and edge effects would definitely enter in. Figure 10 bears this out in that α for the 1-inch cubes is lower than would be expected for paraffin but within experimental error for aluminum.

Thus, the general trends of thermal scattering characterized in Equation 6 seem to be borne out and to comply with theory. Any exact evaluation, especially of the angular variables, requires measurements near θ and θ_0 equal to 90°, and this is experimentally unfeasable. Also, whether Equation 6 or a more accurate analysis, such as one which accounts for absorption (see Y. T. Song's report,[6] which unfortunately has no thermal values of α), should be used can only be decided by much more refined work.

ERRORS

Several sources of errors are present:

1. Statistical fluctuations of the count rates are on the order of the square root of the number counted divided by the time. This error was reduced in some cases by averaging a number of readings, increasing N_o, and increasing the time observed. The error bars on the graphs represent the statistical fluctuation of the count rates.
2. Edge effects as θ becomes large make values for α far from the normal drop drastically.
3. Geometric errors in measuring dimensions account for 8% to 10% error. The greatest of these is the detector diameter and the inside diameter of the collimator.
4. Divergences of the beam for the geometry involved varied by less than 0.5%.

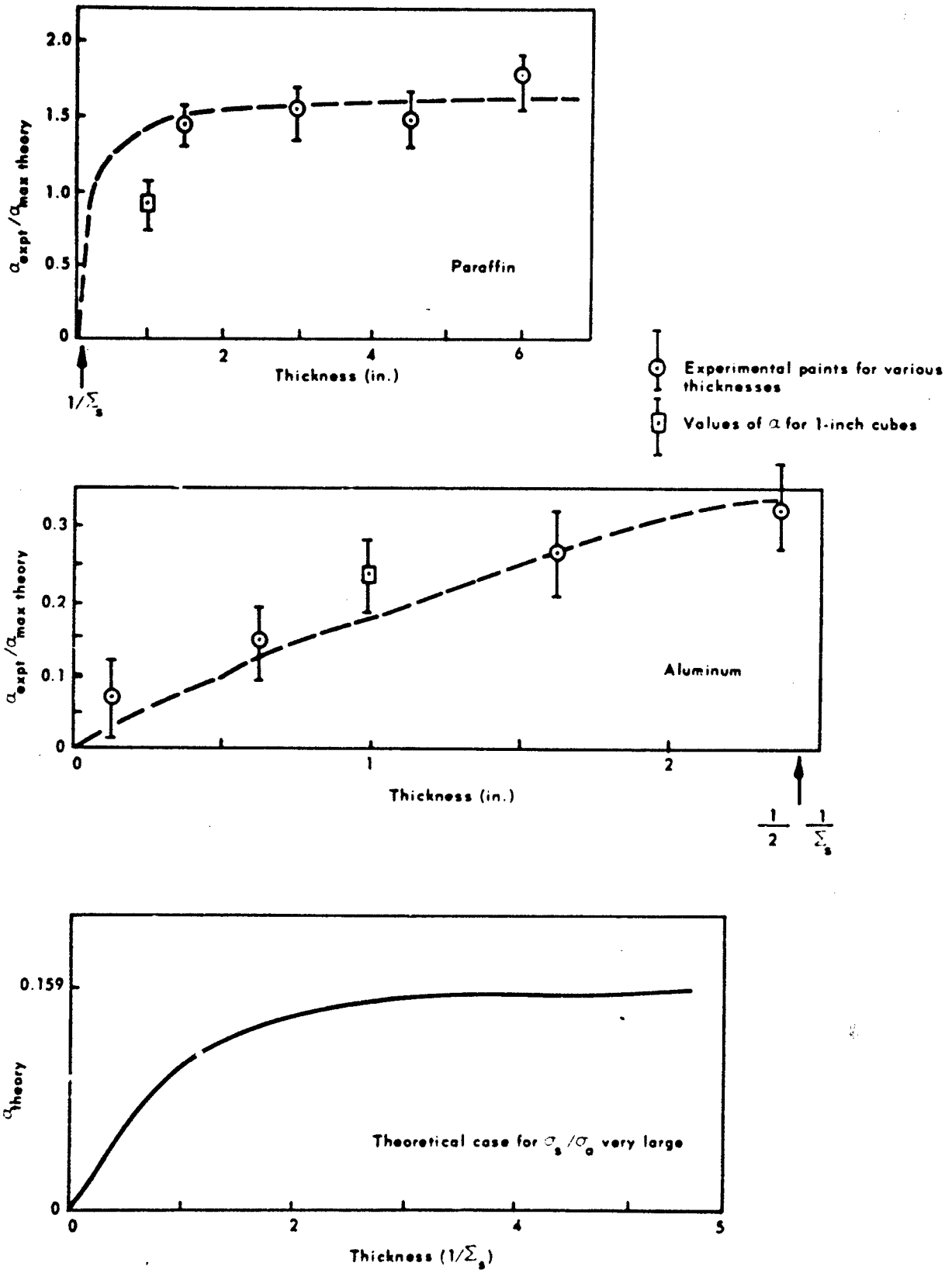

Figure 10. Albedo versus scattering thickness.

FINDINGS AND CONCLUSIONS

The measurements of absolute values of thermal neutron albedo for lead, iron, paraffin, aluminum, carbon, and high-density concrete showed reasonable agreement with theoretical expectations. Deviations from theory were accounted for by geometrical factors inherent in the experimental arrangement. It is, therefore, reasonable to use a simple empirical equation for albedo calculations of thermal-neutron streaming through ducts. Such work is presently being attempted.

The validity of this simple method for cases of grazing incidence cannot be determined without more detailed experimental investigation.

ACKNOWLEDGMENTS

The author wishes to express his thanks to Dean Hicks of the University of California at Los Angeles Engineering Department and to Messrs J. M. Chapman and Y. T. Song of the U. S. Naval Civil Engineering Laboratory for many useful suggestions. Messrs R. McLain, J. Horner, D. Davis, and T. Zane of the UCLA Engineering Reactor Staff helped with many aspects of the experiment.

Table I. Counting Data for Lead (2 inches thick)

$\theta_o = 45^o$	
Angle θ	C (counts/min)
-45	24
-33	38
-22	42
-10	32
0	30
+10	38
+22	35
+33	54
+45	45
+55	56
+60	40

$\theta_o = 0^o$	
Angle θ	C (counts/min)
0	37
+10	41
+22	49
+33	44
+45	52
+50	46
+60	56
+70	49
+80	48

(a) $C_o = 5.27 \times 10^4$ counts/min at 100 watts

(b) Background as a function of angle removed from all counts/min

Table II. Counting Data for High-Density Concrete (2 inches thick)

$\theta_o = 45^\circ$	
Angle θ	C (counts/min)
-45	85
-40	538
-35	269
-30	240
-25	237
-20	235
-15	205
-10	222
-5	227
0	239
+5	270
+10	235
+15	250
+20	219
+25	272
+30	237
+35	232
+40	261
+45	258
+50	291

$\theta_o = 0^\circ$	
Angle θ	C (counts/min)
+15	262
+25	267
+30	307
+35	269
+40	272
+45	331
+50	244
+55	303
+60	276
+65	300
+70	275
$\theta_o = 68^\circ$	
+30	69
+40	54
+45	75
+50	94

(a) $C_o = 2.58 \times 10^5$ counts/min at 500 watts

(b) Data for $\theta_o = 45^\circ$ averaged for 2 min at each angle

Table III. Counting Data for Iron (1 inch thick)

$\theta_o = 45^o$	
Angle θ	C (counts/min)
-30	114
-20	131
-10	104
0	123
+10	109
+20	136
+30	119
+40	141
+50	131

$\theta_o = 0^o$	
Angle θ	C (counts/min)
+15	182
+25	177
+35	159
+45	168
+55	157
+65	153
+75	151

$C_o = 3.34 \times 10^5$ counts/min at 500 watts

Table IV. Counts Versus Thickness for Paraffin, Aluminum, and Carbon

Material	Thickness (in.)	C (counts/2 min)
Paraffin	1.5	927
	3	984
	4.5	941
	6	1,021
Aluminum	0.125	45
	0.625	94
	1.625	168
	2.25	205
Carbon	4	775

(a) $C_o = 8.38 \times 10^5$ counts/2 min at 500 watts

(b) Background = 44 counts/2 min

(c) $\theta_o = 45^\circ$ and $\theta = 0^\circ$ in all cases

Table V. Counts for Various 1-inch Cubes

Material	C (counts/5 min)
Carbon	355
Aluminum	235
Paraffin	914
Lead	177

C_o(calculated) = 2.5 x 2 x 8.38 x 10^5 = 41.9 x 10^5 counts/min at 1,000 watts

Table VI. Albedo Versus Thickness for Paraffin, Aluminum, and Carbon

Material	Thickness (in.)	Albedo
Paraffin	1.5	0.230
	3	0.243
	4.5	0.232
	6	0.276
Aluminum	0.125	0.0111
	0.675	0.0232
	1.625	0.0416
	2.25	0.0510
Carbon	4	0.192

(a) C_o = 8.38 x 10^5 counts/2 min at 500 watts

(b) θ_o = 45° and θ = 0° in all cases

Table VII. Albedo Values for Various 1-inch Cubes

Material	Albedo
Carbon	0.0630
Aluminum	0.0417
Paraffin	0.162
Lead	0.0314

(a) Counts made for 5 min at 1,000 watts

(b) $N = (N_o/R^2)\,\alpha$

$R = 16.5 + 10.75 = 27.25$ in.

$\alpha = (N/N_o)\,7.42 \times 10^2 = N \times 1.772 \times 10^{-4}$

Table VIII. Variation of Albedo With the Ratio σ_s/σ_a

Material	Scattering Length $[1/\Sigma_s]$ (in.)	σ_s/σ_a	α_{expt}	α_{theory} [1]
Carbon	0.81	1,300	~0.19	0.16
Aluminum	4.7	5.8	>0.055	0.054
Iron	0.42	4.2	~0.067	0.048
Lead	1.1	65	~0.11	0.11
Paraffin	0.13	1,200	~0.24	0.16
Concrete	0.95	>1,000	~0.16	0.16

[1] Derived from Reference 7

REFERENCES

1. C. D. Goodman, ed. The science and engineering of nuclear power, vol. 2, ch. 7. Reading, Mass., Addison-Wesley, 1949.

2. S. Glasstone and M. C. Edlund. The elements of nuclear reactor theory. New York, Van Nostrand, 1952, pp. 129-136.

3. E. Amaldi and E. Fermi. "On the absorption and the diffusion of slow neutrons," Physical Review, 2nd Series, vol. 50, Nov. 15, 1936, pp. 899-928.

4. U. S. Naval Civil Engineering Laboratory. Technical Report R-282: Dose measurements for neutron streaming in ducts, by D. R. Doty. Port Hueneme, Calif., Mar. 1964.

5. Radiation Research Associates, Inc. Report RRA-M44: Reflection of thermal neutrons and neutron-capture gamma rays from concrete, by M. B. Wells. Fort Worth, Tex., June 1964.

6. U. S. Naval Civil Engineering Laboratory. Technical Note N-589: A semi-empirical formula for differential dose albedo for neutrons on concrete, by Y. T. Song. Port Hueneme, Calif., Mar. 1964.

7. P. Rafalski. "Evaluation of albedo of neutrons for a slab wall," Nuclear Science and Engineering, vol. 19, no. 3, July 1964, pp. 378-380.

DISTRIBUTION LIST

SNDL Code	No. of Activities	Total Copies	
	1	10	Chief, Bureau of Yards and Docks (Code 42)
23A	1	1	Naval Forces Commanders (Taiwan only)
39B	2	2	Construction Battalions
39D	5	5	Mobile Construction Battalions
39E	3	3	Amphibious Construction Battalions
39F	1	2	Construction Battalion Base Units
A2A	1	1	Chief of Naval Research - Only
A3	2	2	Chief of Naval Operation (OP-07, OP-04)
A5	5	5	Bureaus
B3	2	2	Colleges
E4	1	2	Laboratory ONR (Washington, D. C. only)
E5	1	1	Research Office ONR (Pasadena only)
E16	1	1	Training Device Center
F9	7	7	Station – CNO (Boston; Key West; San Juan; Long Beach; San Diego; Treasure Island; and Rodman, C. Z. only)
F17	7	7	Communication Station (San Juan; San Francisco; Pearl Harbor; Adak, Alaska; Guam; Stockton; and Cheltanham only)
F41	1	1	Security Station
F42	1	1	Radio Station (Oso and Cheltanham only)
F61	2	2	Naval Support Activities (London and Naples only)
F77	1	1	Submarine Base (Groton, Conn. only)
F81	2	2	Amphibious Bases
H3	7	7	Hospital (Chelsea; St. Albans, Portsmouth, Va.; Beaufort; Great Lakes; San Diego; and Camp Pendleton only)
H6	1	1	Medical Center
J1	2	2	Administration Command and Unit – BuPers (Great Lakes and San Diego only)
J3	1	1	U. S. Fleet Anti-Air Warfare Training Center (Virginia Beach only)
J19	1	1	Receiving Station (Brooklyn only)
J34	1	1	Station – BuPers (Washington, D. C. only)

DISTRIBUTION LIST (Contd)

SNDL Code	No. of Activities	Total Copies	
J46	1	1	Personnel Center
J48	1	1	Construction Training Unit
J60	1	1	School Academy
J65	1	1	School CEC Officers
J84	1	1	School Postgraduate
J90	1	1	School Supply Corps
J95	1	1	School War College
J99	1	1	Communication Training Center
L1	11	11	Shipyards
L7	4	4	Laboratory – BuShips (New London; Panama City; Carderock; and Annapolis only)
L26	4	4	Naval Facilities – BuShips (Antigua; Turks Island; Barbados; and Eleuthera only)
L42	2	2	Fleet Activities – BuShips
M27	4	4	Supply Center
M28	6	6	Supply Depot (except Guantanamo Bay; Subic Bay; and Yokosuka)
M61	2	2	Aviation Supply Office
N1	6	18	BuDocks Director, Overseas Division
N2	8	24	Public Works Offices
N5	3	9	Construction Battalion Center
N6	5	5	Construction Officer-in-Charge
N7	1	1	Construction Resident-Officer-in-Charge
N9	6	12	Public Works Center
N14	1	1	Housing Activity
R9	2	2	Recruit Depots
R10	2	2	Supply Installations (Albany and Barstow only)
R20	1	1	Marine Corps Schools (Quantico)
R64	3	3	Marine Corps Base
R66	1	1	Marine Corps Camp Detachment (Tengan only)
W1A1	6	6	Air Station

DISTRIBUTION LIST (Contd)

SNDL Code	No. of Activities	Total Copies	
W1A2	33	33	Air Station
W1B	7	7	Air Station Auxiliary
W1C	3	3	Air Facility (Phoenix; Naha; and Naples only)
W1E	6	6	Marine Corps Air Station (except Quantico)
W1H	9	9	Station – BuWeps (except Rota)
	1	1	Office of the Chief of Engineers, Engineering Division, Civil Works, Department of the Army, Washington, D. C. 20315
	1	1	Chief of Engineers, Department of the Army, Civil Works Directorate, Attn: ENGCW-OE, Washington, D. C.
	1	1	Headquarters, U. S. Air Force, Directorate of Civil Engineering, Attn: AFOCE-ES, Washington, D. C. 20330
	1	1	Commanding Officer, U. S. Naval Construction Battalion Center, Attn: Material Department, Code 140, Port Hueneme, Calif. 93041
	1	1	Director, Coast & Geodetic Survey, U. S. Department of Commerce, 6001 Executive Boulevard, Rockville, Md. 20852
	1	20	Defense Documentation Center, Building 5, Cameron Station, Alexandria, Va.
	1	1	Director of Defense Research and Engineering, Room 3C-128, The Pentagon, Attn: Technical Library, Washington, D. C. 20301
	1	1	U. S. Bureau of Reclamation, Department of Interior, Attn: Mr. T. W. Mermel, Washington, D. C. 20240
	1	1	Facilities Officer, Code 108, Office of Naval Research, Washington, D. C.
	1	1	Commander Naval Beach Group Two, Attn: Project Officer, U. S. Naval Amphibious Base, Little Creek, Norfolk, Va.
	1	1	U. S. Army Engineer Research and Development Laboratories, Attn: STINFO Branch, Fort Belvoir, Va.
	1	1	Air Force Weapons Laboratory, Kirtland Air Force Base, Albuquerque, N. M., Attn: Code WLRC
	1	1	Library, Department of Meteorology and Oceanography, U. S. Naval Postgraduate School, Monterey, Calif.
	1	2	Library of Congress, Washington, D. C.
	1	50	Chief, Input Section, Clearinghouse for Federal Scientific and Technical Information, CFSTI, Sills Building, 5285 Port Royal Road, Springfield, Va. 22151